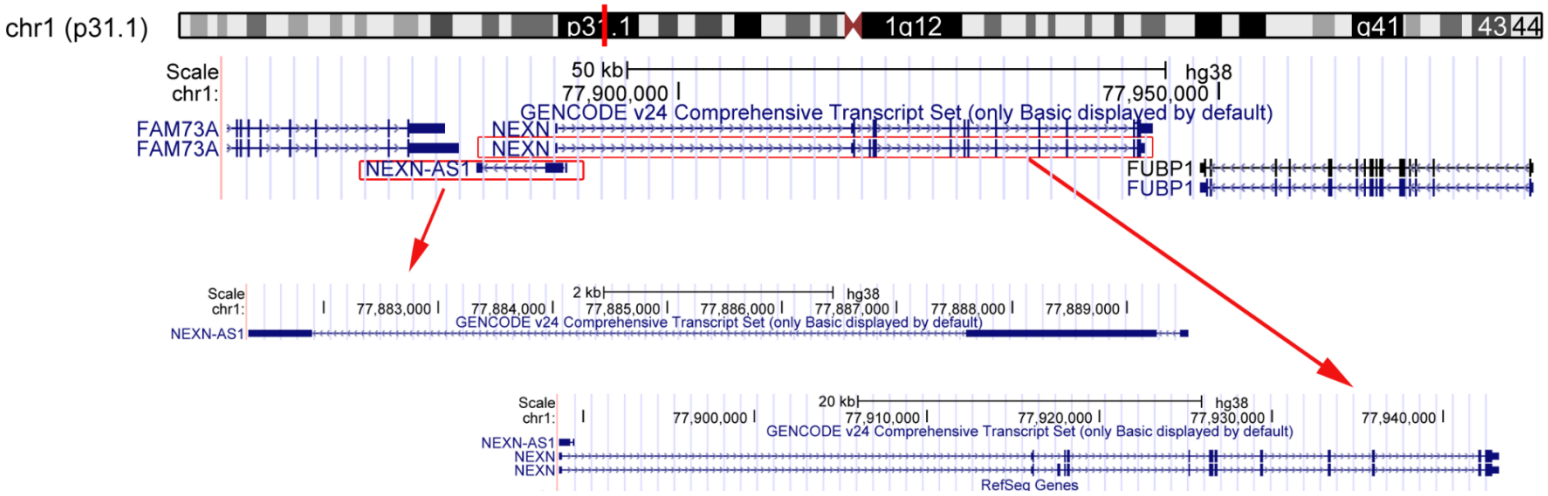

Supplementary Figure S1.

Diagram showing the genomic locations of *NEXN-AS1* and *NEXN*, and their opposite transcriptional directions

Information obtained from University of California Santa Cruz (UCSC) Genome Browser

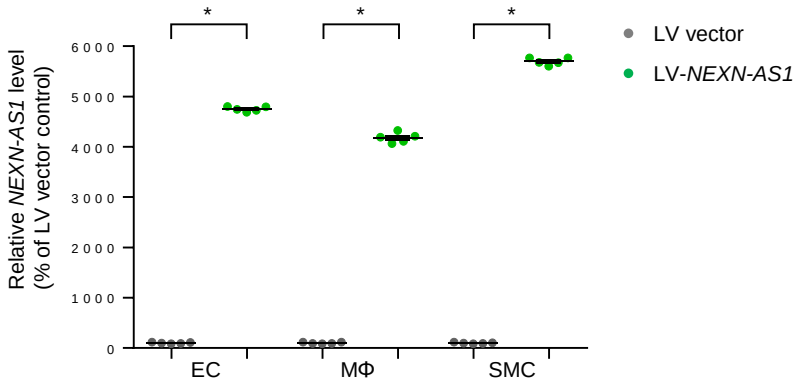

Supplementary Figure S2.
Verification of significant augmentation of *NEXN-AS1* expression in cells transduced with an *NEXN-AS1* expressing lentivirus

Cultured human endothelial cells (EC), macrophages (MΦ), and vascular smooth muscle cells (SMC) were transduced with either an *NEXN-AS1* expressing lentivirus (LV-*NEXN-AS1*) or the lentivirus vector (LV vector) to serve as a control, followed by quantitative RT-PCR analysis of *NEXN-AS1* mRNA levels. Data shown are mean ± SD values in five experiments, *$p<0.001$ by t-test.

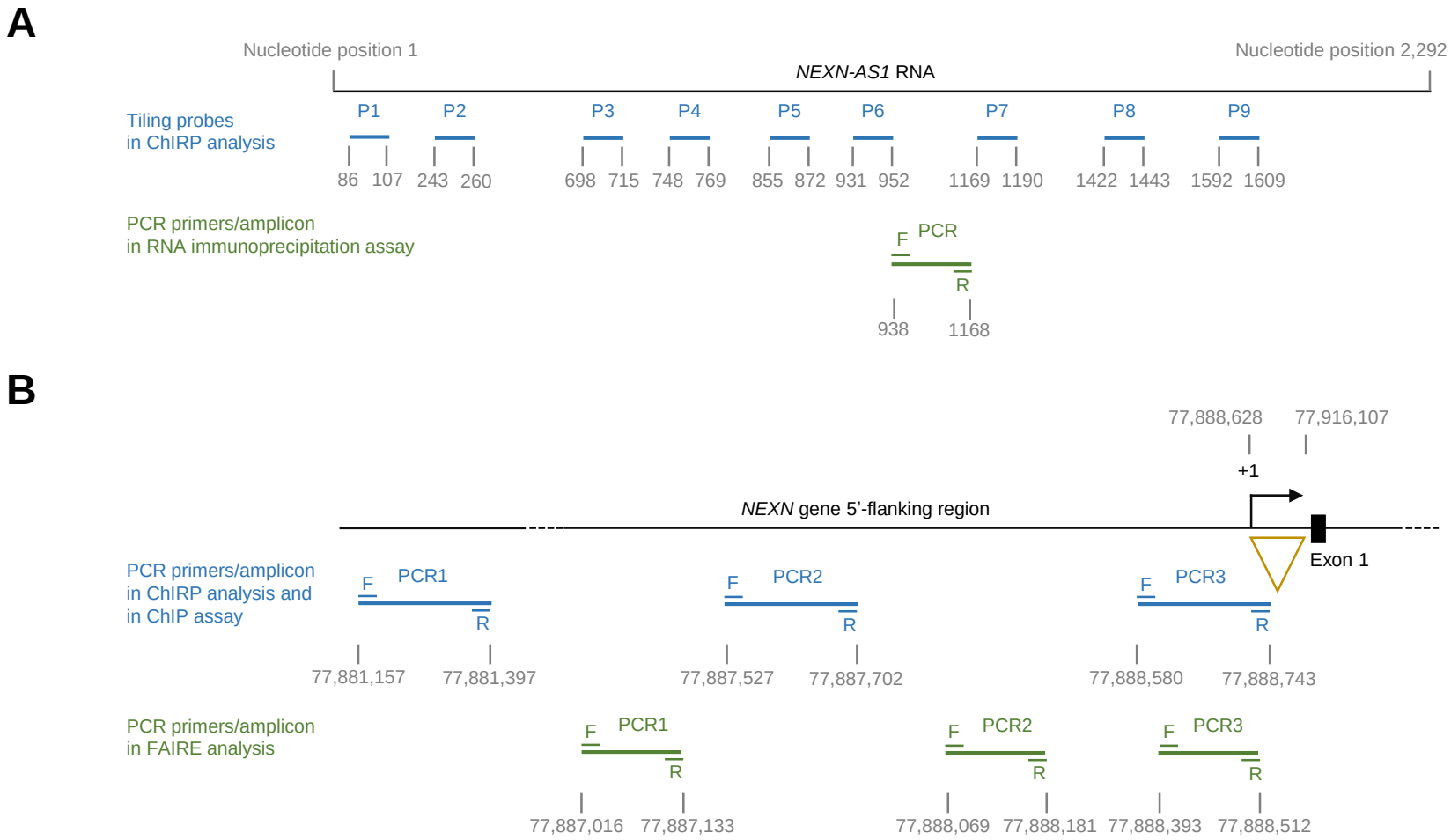

Supplementary Figure S3

A. Schematic representation of positions of antisense DNA tiling probes (P1 to P9) for pulldown of *NEXN-AS1* in ChIRP (chromatin isolation by RNA purification) analysis and position of PCR primers to detect *NEXN-AS1* in RNA immunoprecipitation assay.
B. Schematic representation of positions of PCR primers used to detect *NEXN* gene 5'-flanking region in ChIRP analysis, ChIP (chromatin immunoprecipitation) assay, and FAIRE (formaldehyde-assisted isolation of regulatory elements) analysis, respectively. The numbers 77,881,157, etc, indicate nucleotide positions on chromosome 1 in human genome assembly CRCh38/hg38. Triangle indicates deleted region in the luciferase reporter assay.
F: forward primer; R: reverse primer.

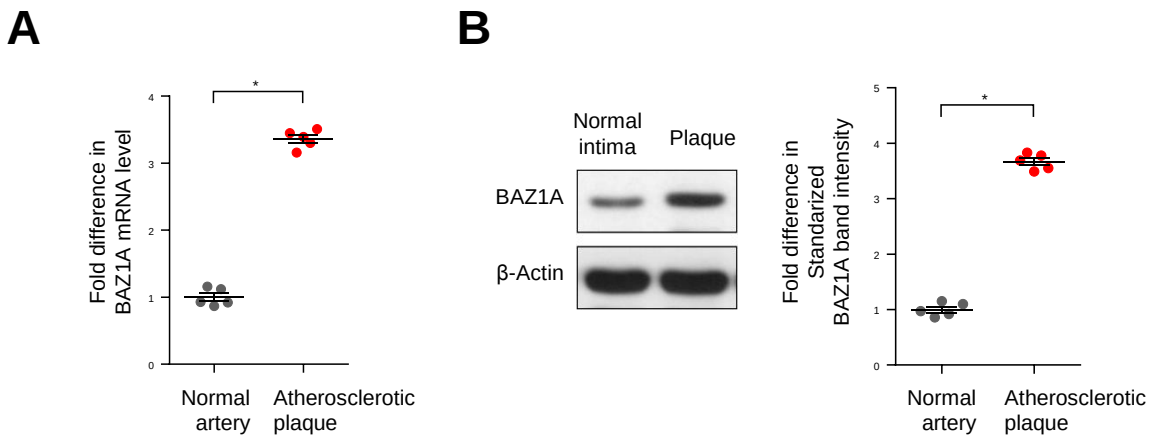

Supplementary Figure S4.

Atherosclerotic plaques have higher levels of BAZ1A than normal artery

Human atherosclerotic plaques and normal arterial tissues were subjected to quantitative RT-PCR and immunoblot analyses of BAZ1A. **A.** Fold difference in BAZ1A mRNA level between atherosclerotic plaques and arterial tissues. **B.** Left, representative immunoblot images; right, fold difference (mean ± SD) in BAZ1A band intensity standardized against β-actin band intensity. n=5 subjects in each group, *p<0.001 by t-test.

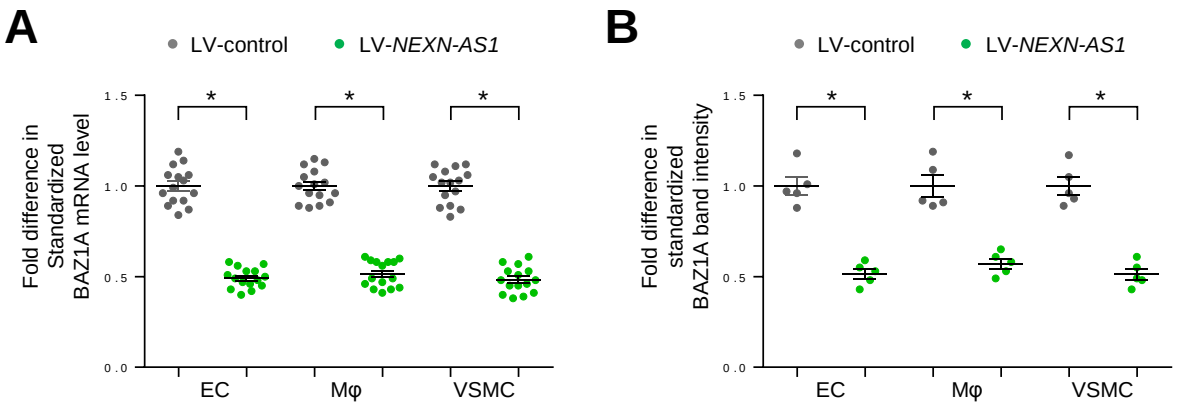

Supplementary Figure S5.
***NEXN-AS1* suppresses BAZ1A expression**

Cultured human endothelial cells (EC), macrophages (MΦ), and vascular smooth muscle cells (SMC) were transduced with either an *NEXN-AS1* expressing lentivirus (LV-*NEXN-AS1*) or the lentivirus vector (LV vector) to serve as a control, followed by quantitative RT-PCR and immunoblot analyses of BAZ1A. **A.** Fold differences (mean ± SD) in BAZ1A mRNA level between the two groups in five independent experiments with triplicates in each experiment. **B.** Left, representative immunoblot images; right, fold difference (mean ± SD) between the two groups in BAZ1A band intensity standardized against β-actin band intensity in five independent experiments, *$p<0.05$ by t-test.

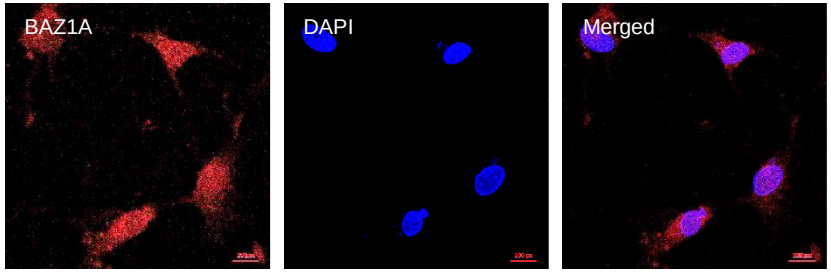

Supplementary Figures S6
Immunofluorescence analysis showing the presence of BAZ1A in both the cytoplasm and nucleus of cultured vascular endothelial cells

Cultured human vascular endothelial cells were subjected in immunofluorescence microscopy. BAZ1A was stained red using an anti-BAZ1A antibody and the nucleus stained blue with 4',6-diamidino-2-phenylindole (DAPI). Images shown are in 100×magnification.

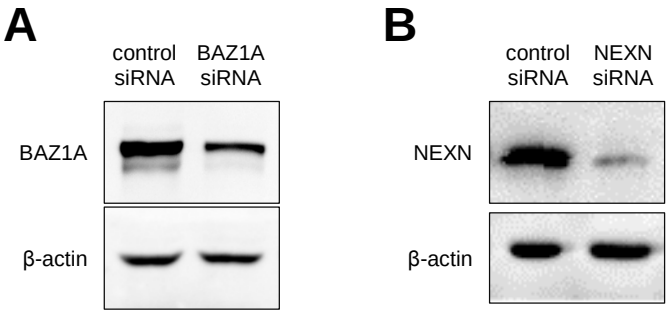

Supplementary Figure S7.
Verification of siRNA-mediated knockdown of BAZ1A and NEXN, respectively
Cultured human vascular endothelial cells were transduced with either a BAZ1A siRNA or a scramble (control) siRNA (**A**), or with either an NEXN siRNA or a scramble (control) siRNA (**B**). Transfected cells were subjected to immunoblot analysis of either BAZ1A (**A**), NEXN (**B**), or the housekeeping protein β-actin as a protein loading control (**A** and **B**).

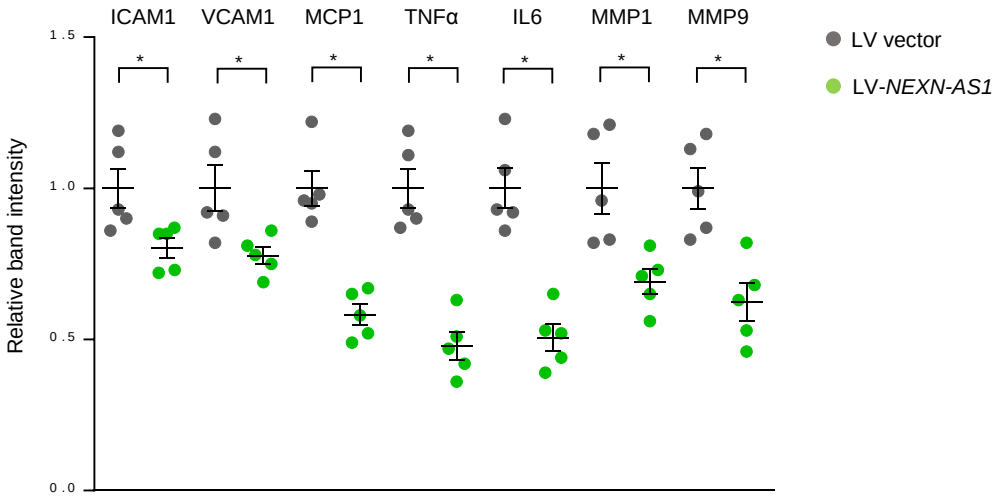

Figure S8. *NEXN-AS1* inhibits the expression of inflammatory molecules

Cultured human vascular endothelial cells were transfected with either an *NEXN-AS1*-expressing lentivirus (LV-*NEXN-AS1*) or the lentivirus vector (LV vector) to serve as a control, then stimulated with lipopolysaccharides (1μg/ml) for 12 hours, followed by immunoblot analysis. Shown in this figure are fold differences between the two groups in ICAM1, VCAM1, MCP1, TNFα, IL6, MMP1, and MMP9 band intensities, respectively, standardized against band intensity of the housekeeping protein β-actin, in five independent experiments. Column chart shows fold differences (mean ±SD) in five experiments, *p<0.05 by t-test.

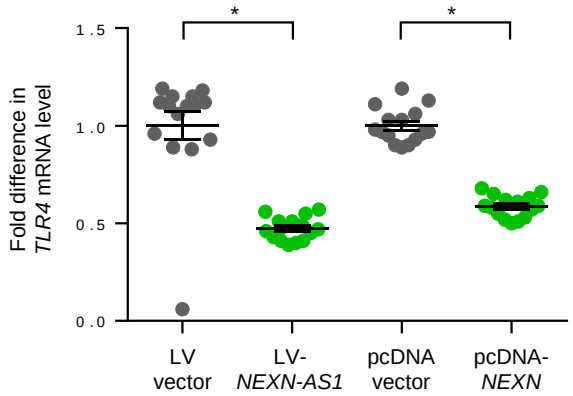

Supplementary Figure S9.
***NEXN-AS1* and NEXN suppress TLR4 expression**

Cultured human endothelial cells were transfected with either an *NEXN-AS1* expressing lentivirus (LV-*NEXN-AS1*), the lentivirus vector (LV vector), an NEXN expressing plasmid (pcDNA-NEXN) or the plasmid vector (pcDNA vector), followed by quantitative RT-PCR analysis of TLR4. Column charts shows fold differences (mean ± SD) in TLR4 mRNA level in five independent experiments with triplicates in each experiment, *$p<0.05$ by t-test.

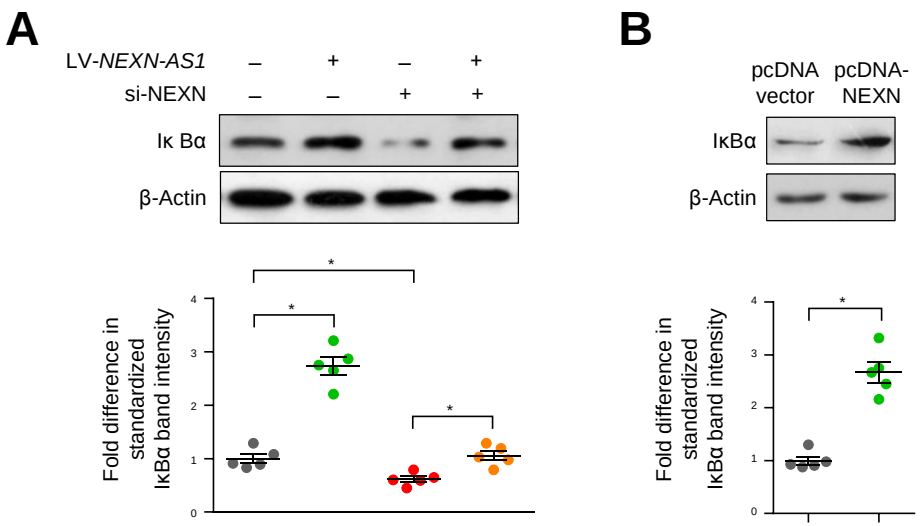

Figure S10. *NEXN-AS1* and NEXN increase the levels of the NFκB inhibitor, IκBα

A. Cultured human vascular endothelial cells were transfected with an *NEXN-AS1*-expressing lentivirus (LV-*NEXN-AS1*), the lentivirus vector (LV vector) to serve as a control, an NEXN siRNA to knock down NEXN, and/or a control siRNA, then stimulated with lipopolysaccharides (1μg/ml) for 12 hours, followed by immunoblot analysis of IκBα.

B. same as **A**, except that cells were transfected with either a plasmid (pcDNA-NEXN) to overexpression or the plasmid vector (pcDNA vector), instead. Top: representative immunoblot images; bottom: fold differences in IκBα band intensity standardized against β-actin band intensity. Data shown in the column charts are mean ± SD values in five independent experiments, *p<0.05 by ANOVA with post hoc analysis and Bonferroni correction (**A**) or t-test (**B**).

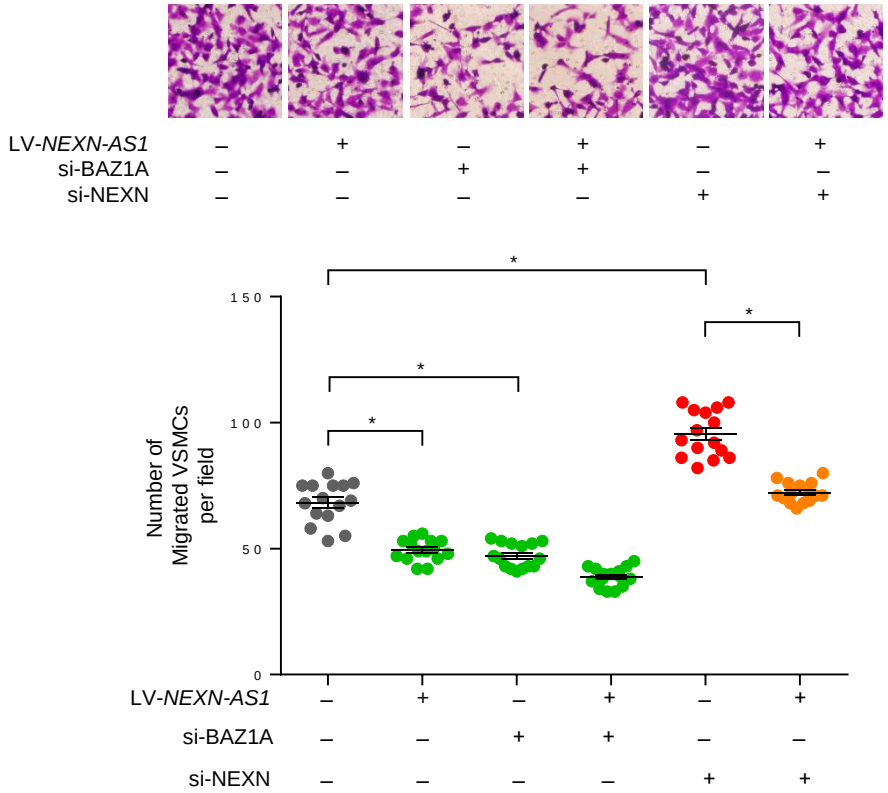

Supplementary Figure S11.

***NEXN-AS1* and NEXN inhibit vascular smooth muscle cell migration**

Cultured human vascular smooth muscle cells were transfected with either an *NEXN-AS1* expressing lentivirus (LV-*NEXN-AS1*), BAZ1A siRNA (si-BAZ1A) or NEXN siRNA (si-NEXN), followed by a migration assay using the transwell method. Images show migrated vascular smooth muscle cells, in 100× magnification.. Column charts shows fold differences (mean ± SD) in migrated cells per microscopic field in five independent experiments with triplicates in each experiment, *p<0.05 by ANOVA with post hoc analysis and Bonferroni correction.

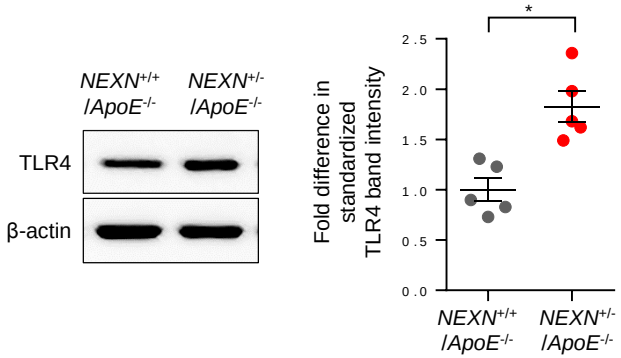

Supplementary Figure S12. NEXN deficiency increases TLR4 level

NEXN$^{+/-}$*/ApoE*$^{-/-}$ mice and *NEXN*$^{+/+}$*/ApoE*$^{-/-}$ littermates, six weeks of age, were fed a Western high-fat diet for 12 weeks, followed by immunoblot analysis of TLR4 in aortic tissues. Left: representative immunoblot images; right: fold differences in TLR4 band intensity standardized against β-actin band intensity. Data shown in the column charts are mean ± SD values, n=5 animals in each group, *$p<0.05$ by t-test.

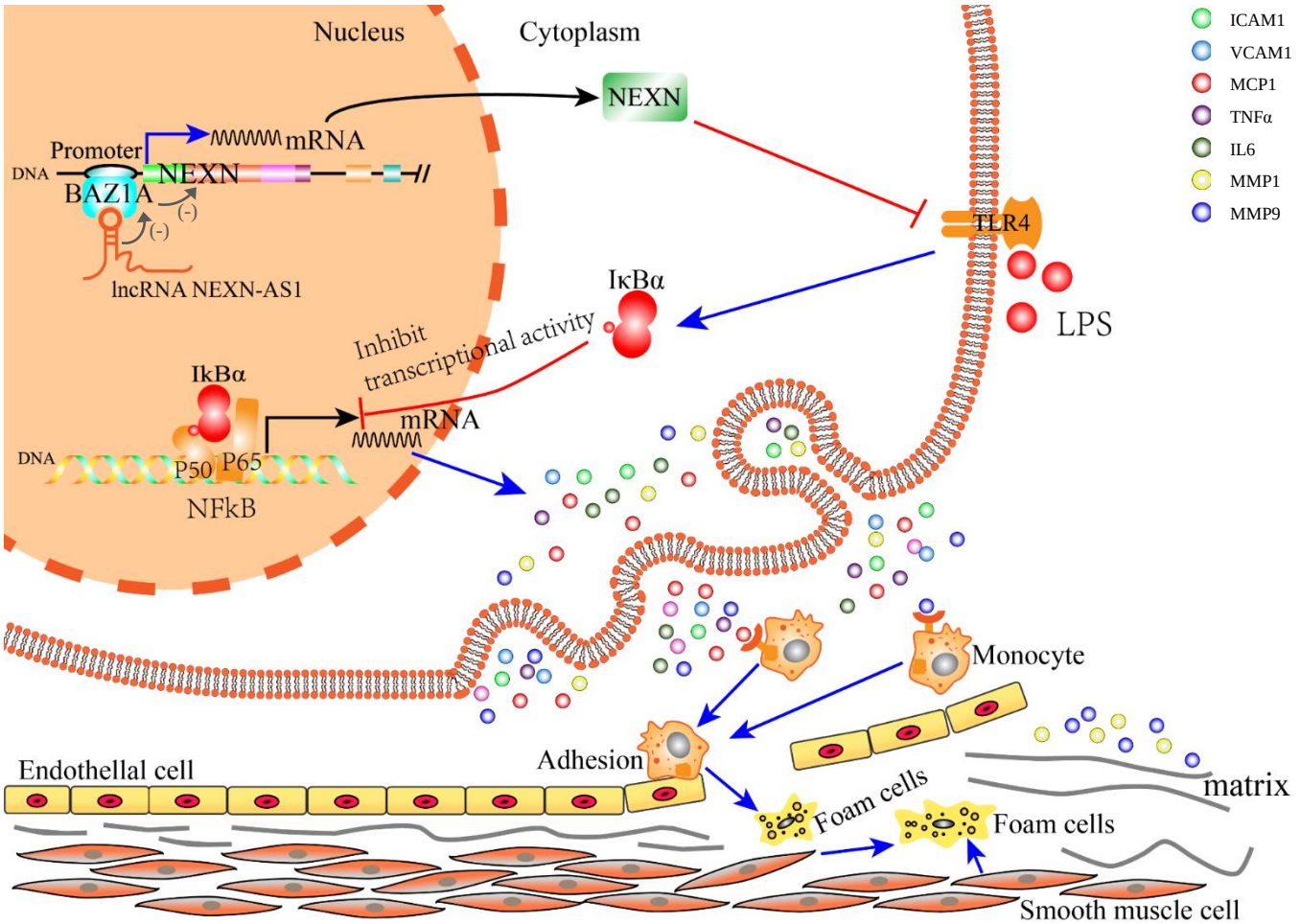

Supplementary Figure S13. Schematic presentation of the anti-atherogenic roles of *NEXN-AS1* and NEXN
The results of the present study indicate that: 1) the lncRNA *NEXN-AS1* interacts with the chromatin remodeler BAZ1A and upregulates NEXN; 2) NEXN inhibits the TLR4 pathway, suppresses NFκB activity, and reduces the expression of adhesion molecules (ICAM1, VCAM1, and MCP1), inflammatory cytokines (TNFα and IL6) and matrix metalloproteinases (MMP1 and MMP9); 3) NEXN attenuates monocyte adhesion to endothelial cells; and 4) NEXN plays a protective role against atherosclerosis.

Supplementary Table 3.

Proteins identified by protein mass spectrometric analysis of the chromatin complex pulled down by *NEXN-AS1* RNA probes

Protein		Main function
ACTB	Actin, cytoplasmic	Structural protein
ANR63	Ankyrin repeat domain-containing protein 63	Protein interaction
BAZ1A	Bromodomain adjacent to zinc finger domain protein 1A	Chromatin remodeling and gene regulation
H2A1A	Histone H2A type 1-A	DNA binding
H4	Histone H4	DNA binding
HNRPM	Heterogeneous nuclear ribonucleoprotein M	mRNA processing
HNRPU	Heterogeneous nuclear ribonucleoprotein U	mRNA processing
HS90B	Heat shock protein HSP 90-beta	Protein processing
HSP7C	Heat shock cognate 71 kDa protein	Protein processing
K1C18	Keratin, type I cytoskeletal 18	Structural protein
K2C7	Keratin, type II cytoskeletal 7	Structural protein
K2C8	Keratin, type II cytoskeletal 8	Structural protein
KPYM	Pyruvate kinase PKM	Carbohydrate metabolism
LMNA	Prelamin-A/C	Nucleus organization
MYH10	Myosin-10	Structural protein
MYH9	Myosin-9	Structural protein
NUCL	Nucleolin	Ribosome maturation
PADI2	Protein-arginine deiminase type-2	Chromatin organization
TBA1B	Tubulin alpha-1B chain	Structural protein
TBB5	Tubulin beta chain	Structural protein
TCPZ	T-complex protein 1 subunit zeta	Protein processing
TRAP1	Heat shock protein 75 kDa, mitochondrial	Protein processing
VIME	Vimentin	Structural protein

Supplementary Table 4.

Demographic, clinical and biochemical characteristics of study subjects

	Healthy control (n=40)	CCHD (n=113)	AMI (n=69)	HF (n=41)
Age (years)	51.5±8.5	54.8±7.9	53.7±9.5	49.6±8.9
Male/female (n/n)	23/17	63/50	31/38	25/16
Total cholesterol (mmol/L)	4.49±0.51	4.42±1.28	4.80±1.32	3.61±1.03*#
Low density lipoprotein (mmol/L)	2.60±0.34	2.78 ±0.96	3.08±1.10	2.26±0.57 #
High density lipoprotein (mmol/L)	1.31±0.15	1.05±0.31*	1.00±0.26*	1.07±0.31*
Total triglyceride (mmol/L)	0.98±0.34	1.54±0.89*	1.56±0.89*	1.23±0.78
Apolipoprotein A1 (g/L)	1.43±0.36	1.20±0.23*	1.18±0.27*	1.13±0.21*
Apolipoprotein B (g/L)	0.80±0.18	0.88±0.30	0.96±0.30	0.77±0.20
Lipoprotein (a) (g/L)	0.13 (0.02, 0.23)	0.79 (0.03, 1.22)*	0.34 (0.04, 0.64) *	0.22 (0.01, 0.42)
Homocysteine (μmol/L)	21.59±4.48	19.90±7.12	18.80±7.51	22.01±5.73
Myoglobin (ng/mL)	27.23 (19.68, 48.57)	85.33 (30.89, 311.02)#	159 (29.38, 1596.87)*	107.49 (25.18, 289.73)
Troponin I (ng/mL)	0.01 (0.00, 0.01)	1.51 (0.00, 6.78)#	8.51 (0.43, 48.79)*	0.11 (0.00, 0.43)#
Creatine phosphokinase (IU/L)	78 (9, 153)	275 (25, 962)#	1331 (241, 12350)*	109 (33, 256)#
Creatine phosphokinase-MB fraction (IU/L)	18 (2, 24)	28 (5, 96)#	108 (29, 328)*	15 (6, 23)#
C-reactive protein (mg/dL)	1.24 (0.01, 2.38)	15.06 (0.26, 47.86)#	29.73 (6.96, 121.37)*	22.61 (0.12, 85.75)
Lactate dehydrogenase (IU/L)	208 (96, 369)	240 (121, 464)#	466 (120, 1296)*	216.00 (157, 332.)#
Aspartate aminotransferase (IU/L)	23 (5, 38)	48 (6, 159)#	117 (43, 938)*	35 (10, 65)#
NEXN (pg/mL)	393.65±113.87	290.57±152.12*	305.56±137.68 *	283.82±147.33*

Data are presented as mean ± SD or median (interquartile range) unless otherwise indicated.
*indicates $p< 0.05$ compared with healthy control group; #denotes $p< 0.05$ compared with acute myocardial infarction group.
CCHD, chronic coronary heart disease; AMI, acute myocardial infarction; HF, heart failure.

Supplementary Table 5.

Sequences of siRNAs used in this study

Gene name	Target sequences	Sense(5′-3′)	Antisense(3′-5′)
si-h-*NEXN*	GGAGATGATTCACTACTTA	GGAGAUGAUUCACUACUUA dTdT	dTdT CCUCUACUAAGUGAUGAAU
si-h-*BAZ1A*	CCAGCTTATTGAAGCTCTT	CCAGCUUAUUGAAGCUCUU dTdT	dTdT GGUCGAAUAACUUCGAGAA
si-h-*TLR4*	GGAAACTTGGAAAAGTTTG	GGAAACUUGGAAAAGUUUG dTdT	dTdT CCUUUGAACCUUUUCAAAC

h, Human; si, short interfering RNA.

Supplementary Table 6.

Sequences of tiling probes for pulldown of *NEXN-AS1* or control probes used in the ChIRP experiment

Probe ID	5' - 3' sequence
P1	GCAGTGCCAGTTAAGAAATCCT
P2	GTCGGCTGAGTTTCGGGT
P3	CCAGAGGACTCCCAGCGG
P4	ACTTTTATGGAAACTTGCTGCT
P5	ATAACGGCGGAGGTGGGG
P6	GACAAATTCTGGCGGAAAGTTG
P7	GATATGTAGTGGCTTGGCTTCT
P8	CCTCTGCCTTCAACTTTCTTCT
P9	GCTGGCGGTCCAAGTTGA
C1	TCACGACGTTGTAAAACGAC
C2	ATTAAGTTGGGTAACGCCAG
C3	AGGTTACGTTGGTGTAGATG
C4	AATGTGAGCGAGTAACAACC
C5	GTAGCCAGCTTTCATCAACA
C6	AATAATTCGCGTCTGGCCTT
C7	AGATGAAACGCCGAGTTAAC
C8	AATTCAGACGGCAAACGACT
C9	TTTCTCCGGCGCGTAAAAAT
C10	ATCTTCCAGATAACTGCCGT
C11	AACGAGACGTCACGGAAAAT
C12	GCTGATTTGTGTAGTCGGTT

Biotinylated 20mer antisense oligonucleotides were designed using Stellaris single-molecule FISH probe designer software (singlemoleculefish.com).

P1 to P9 are probes for *NEXN-AS1* pulldown; C1 to C12 are control probes targeting *LacZ* mRNA —normally absent in human cells.